PROCEEDINGS OF SCIENCE

Prospects for ultra-high-energy particle acceleration at relativistic shocks

Zhi-Qiu Huang,[a,*] **Brian Reville,**[a] **John G. Kirk**[a] **and Gwenael Giacinti**[b,c,a]

[a] *Max-Planck-Institut für Kernphysik, 69117 Heidelberg, Germany*
[b] *Tsung-Dao Lee Institute, Shanghai Jiao Tong University, Shanghai 201210, P. R. China*
[c] *School of Physics and Astronomy, Shanghai Jiao Tong University, Shanghai 200240, P. R. China*

E-mail: zhiqiu.huang@mpi-hd.mpg.de, brian.reville@mpi-hd.mpg.de

Using test-particle Monte-Carlo simulations, we revisit the particle acceleration at ultra-relativistic shocks. The produced particle spectra are studied on the conditions of two regular field configurations: (i) uniform upstream field perpendicular to the shock normal, and (ii) upstream field with a cylindrical geometry. For uniform field configurations, particles could keep being accelerated until becoming magnetized on either side of the shock, which contradicts the widely-held belief that the maximum energy is constrained by the *downstream magnetized limit*. The corresponding steady-state particle distribution satisfies $dN/d\gamma \propto \gamma^{-2.2}$, similar to that predicted for the parallel shock case. For the cylindrical field configuration, the acceleration efficiency depends on the charge of the particles. Particles with a favorable charge will experience a curvature drift motion parallel to the shock velocity and hence increases the probability of downstream particles to cross the shock. Considering the non-resonant scattering model, these particles can only escape when reaching the confinement limit of the system size, and the accelerated spectrum could become even harder.

38th International Cosmic Ray Conference (ICRC2023)
26 July - 3 August, 2023
Nagoya, Japan

*Speaker

PoS(ICRC2023)193

1. Introduction

Shocks are a universal phenomenon in high-energy astrophysics, which have been observed from many objects like supernovae (SNe) and gamma-ray bursts (GRBs). They have long been considered as one of the most promising mechanisms to accelerate high-energy cosmic rays. Depending on their velocities, shocks can be divided into the non-relativistic and the relativistic case.

At relativistic shocks, particles can gain energy through keeping crossing the shock. Downstream particles have to chase the relativistic shock front. As a result, particles that can return back to upstream are constrained in a cone with a small opening angle $\sim 1/\Gamma_s$, where Γ_s is the Lorentz factor of the shock. To return back to downstream, these particles should change their directions of motion to leave this loss cone.

The downstream magnetic field is almost perpendicular to the shock normal because of shock compression, unless the angle between the regular field and the shock normal in upstream is $\lesssim 1/\Gamma_s$. Particles moving along the magnetic line should be scattered by a large angle of roughly 90° to catch the shock.

There are two mechanisms that can influence the particle trajectory near the shock. Particles would move along the regular field lines and do gyro-motion/regular deflection. Besides, there also exists small-scale magnetic turbulence, which can collide and scatter particles. It is widely accepted that, when the trajectories of downstream particles are dominant by regular deflection, they would be washed away far downstream and cannot be accelerated anymore, providing a limit on the maximum accelerated energy known as the *downstream magnetized limit*.

Using test-particle Monte-Carlo simulations (details seen in Huang et al. [5]), we demonstrate that such a widely-held belief is mis-informed. Uniform and cylindrical magnetic field confugurations are considered in this work. In the following, times and distances are normalized to the non-relativistic gyro-frequency and radius corresponding to the downstream magnetic field B_{0-}. Simulation results are all plotted in the downstream rest frame without additional descriptions.

2. Uniform perpendicular magnetic field

First we consider the case where a uniform upstream magnetic field is perpendicular to the shock normal. This is a generic configuration for relativistic shocks. The downstream field would lie in the plane of the shock and the velocity of the intersection point between the magnetic field line and the shock surface would exceed the speed of light c, unless the upstream regular field is aligned to the shock normal with an angle of $1/\Gamma_{sh}$. In this work we adopt the Lorentz factor of the shock in the upstream rest frame $\Gamma_{sh} = 50\sqrt{2}$ as a constant. Determined by the ideal magnetohydrodynamic shock jump conditions for a weakly magnetized ultra-relativistic shock, the downstream field $B_- = 2\sqrt{2}\Gamma_{sh}B_+$, where $B_\pm$ are the magnetic field measured in the corresponding rest frame [1]. Following Kirk & Reville [2], the scattering frequency of the non-resonant interactions can be characterized as

$$\nu_\pm = \nu_{0\pm}(p/mc)^{-2}. \tag{1}$$

Here we set $\nu_{0-} = 3 \times 10^4 \omega_-$ and treat ν_{0+} as a free parameter.

Achterberg et al. [3] asserted that acceleration at a superluminal, relativistic shock would be inefficient in the absence of strong cross-field diffusion, since the guiding center of a downstream

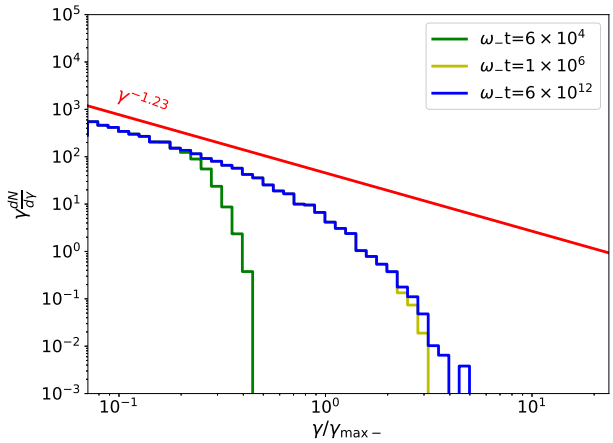

Figure 1: The particle spectra at a perpendicular shock in a uniform magnetic field with relatively weak scattering upstream $\nu_{0+} = 10^{-4}\nu_{0-}$, as a function of the ratio of the Lorentz factor to its predicted maximum, $\gamma_{\rm max-} = \nu_{0-}/\omega_- = 3\times10^4$, see eq (2). The upstream magnetized limit, $\gamma_{\rm max+} \approx 600$, lies close to the injection energy and is not shown.

magnetized particle recedes from the shock front with a velocity comparable to c. Hence, the maximum accelerated energy should be determined by the so-called *downstream magnetized limit*

$$\gamma_{\rm max-} = \nu_{0-}/\omega_-, \tag{2}$$

which is referred in Huang et al. [4].

Similarly it is also possible to define an *upstream magnetized limit* taking account a particle upstream being scattered or deflected through a small angle $\sim 1/\Gamma_{\rm sh}$ before being overtaken by the shock

$$\gamma_{\rm max+} = 2\sqrt{2}\Gamma_{\rm sh}\nu_{0+}/\omega_- \,. \tag{3}$$

For $\nu_{0+} = 10^{-4}\nu_{0-}$, implying $\gamma_{\rm max-} = 3\times10^4$ and $\gamma_{\rm max+} \approx 600 \ll \gamma_{\rm max-}$, the simulations are shown in Fig. 1. When the particle distribution reach a stationary state, the cutoff on the spectrum, which presents the maximum accelerated energy, locates at roughly $\gamma_{\rm max-}$. This is in agreement with the findings in Achterberg et al. [3].

The situation changes if $\gamma_{\rm max+} \gg \gamma_{\rm max-}$. Fig. 2 shows results for $\nu_{0+} = \nu_{0-}$, implying $\gamma_{\rm max-} = 3\times10^4$ and $\gamma_{\rm max+} = 6\times10^6 \gg \gamma_{\rm max-}$. In this case the saturation of acceleration occurs not at $\gamma_{\rm max-}$, but extends to $\gamma_{\rm max+}$.

For a particle with Lorentz factor $\gamma_{\rm max-} \ll \gamma \ll \gamma_{\rm max+}$, its trajectory is dominant by random scattering upstream whilst by regular deflection downstream, as illustrated in Fig. 3.

At time $t = t_0$, this particle is caught by the shock and moves from upstream to downstream, with a phase angle φ. Here $\varphi = 0$ points towards the positive x-axis direction and increases clockwise. At $t = t_1$, this particle is deflected by the regular magnetic field and catches the shock again. Note the particle must catch the shock before its velocity along x-axis β_x becomes smaller than the shock velocity. Hence there exists a critical angle $\theta = \arcsin\left(\frac{1}{3\beta_\perp}\right)$, and particles should

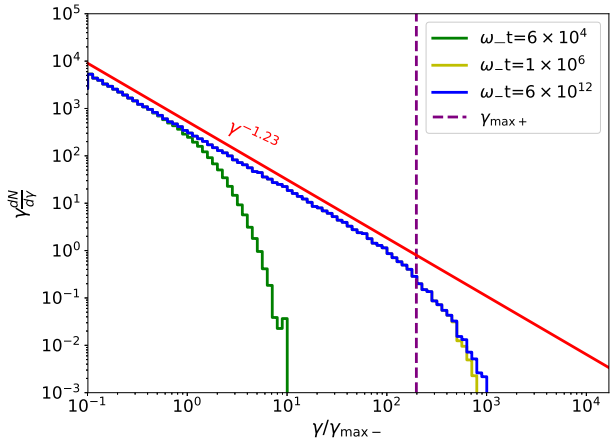

Figure 2: Particle spectra at a perpendicular shock in a uniform magnetic field, with relatively strong scattering upstream: $\nu_{0+} = \nu_{0-}$ and $\nu_{0-}/\omega_- = 3 \times 10^4 = \gamma_{\rm max-}$, plotted as a function of $\gamma/\gamma_{\rm max-}$. The vertical dashed line shows the upstream magnetized limit, $\gamma_{\rm max+}$, see eq (3).

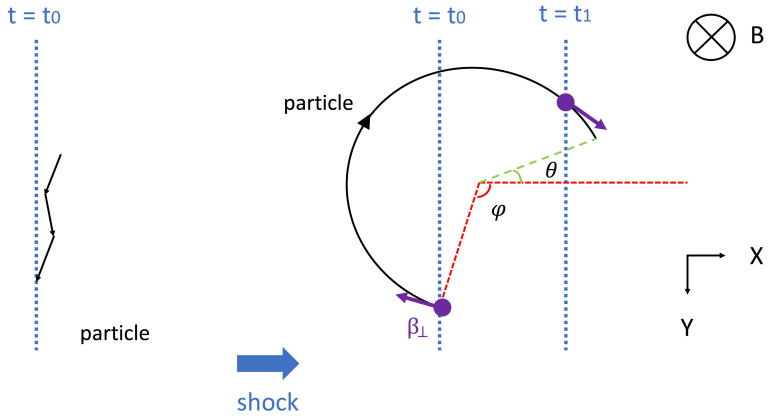

Figure 3: Schematic picture of the particle trajectory in the downstream rest frame. Here we consider an extreme case: pure scattering in upstream and only regular deflection in downstream. The shock moves along the x-axis and the regular magnetic field points toward the z-axis. A particle with negative charge would rotate along the field clockwise. At $t = t_0$, the particle is caught by the shock and moves from upstream to downstream. At $t = t_1$, this particle catch the shock by regular deflection and moves from downstream to upstream. $\beta_\perp$ is the particle velocity perpendicular to the regular field, φ represents the initial phase when the particle moves to downstream, and θ represents the angle in which the particle velocity along the x-axis become smaller than the shock velocity.

catch the shock front before moving into this angle. For particles that can return back to upstream by regular deflection, the relation between $\beta_\perp$ and φ is written as:

$$\frac{(\cos\theta - \cos\varphi)r_g}{c/3} > \frac{2\pi - \varphi - \theta}{\omega_g}. \tag{4}$$

where $r_g = \beta_\perp/\omega_g$. Note $\varphi \leqslant 2\pi - \theta$.

Besides, when the particle moves from upstream to downstream at $t = t_0$, its velocity along x-axis must be smaller than the shock velocity,

$$\beta_x < \frac{1}{3}. \tag{5}$$

More corresponding details are analyzed in Kirk et al. [6], where both the Monte-Carlo code in this work and an analytical approximation method are used. For ultra-relativistic shocks, stationary spectra satisfying $dN/d\gamma \propto \gamma^{-2.17}$ can be found in the regime $\gamma_{\rm max-} \ll \gamma \ll \gamma_{\rm max+}$, quite close to that in the strictly parallel shock case.

3. Cylindrical magnetic field

Despite the assumption of a uniform perpendicular is generic, a magnetic field with cylindrical symmetry is more realistic in high-energy astrophysics, i.e., to model a reverse shock in a magnetized jet, or the forward shock of a jet propagating into ambient medium that mimics the Parker wind. For simplicity we consider a static field in upstream with only azimuthal components existing in cylindrical coordinates (ρ, θ, x). $\partial B_\theta/\partial\theta = 0$ is required to satisfy the solenoidal field condition. Hence for a cylindrical perpendicular shock,

$$\boldsymbol{B_\pm} = B_{0\pm}\hat{\boldsymbol{\theta}} \times \begin{cases} (\rho/\rho_0), & \rho \leqslant \rho_0 \\ 1, & \rho_0 < \rho \leqslant \rho_{\rm max}\,. \end{cases} \tag{6}$$

We also set a boundary at $\rho = \rho_{\rm max} \gg \rho_0$. All particles are assumed to escape when reaching this boundary. Here we adopt $\rho_0 = 10^5$ and $\rho_{\rm max} = 10^7$. $\Gamma_{\rm sh} = 50\sqrt{2}$ and $\nu_{0-} = 3\times10^4\omega_-$ are selected as in section 2.

The corresponding spectra for weak upstream scattering, $\nu_{0+} = 10^{-4}\nu_{0-}$, are shown in Fig. 4. At low energy, particle trajectories in the downstream region are dominated by scattering, so that the spectrum looks similar to Fig. 1. Roughly above the downstream magnetized limit $\gamma_{\rm max-}$, there is a dramatic difference. The blue spectrum for particles with $qB_{0-} < 0$ cuts off, while the yellow one for $qB_{0-} > 0$ hardens to higher energy until being saturated by the confinement limit $\gamma \approx \rho_{\rm max}$.

The positions where particles are initially injected would affect the produced spectrum since particles far from the axis $\rho = 0$ can't benefit from the curvature drift. Such an effect is demonstrated in Fig. 6, where particles are injected uniformly in ρ between the axis and $\rho_{\rm max}$. Only a small fraction of particles that are sufficiently close to the axis can achieve a substantial drift velocity for further acceleration, which causes a soft part before the spectrum hardening. Note that in Fig. 6, $\rho_{\rm max}$ is reduced by a factor of 2 compared to what we used in Fig. 4, hence the maximum energy decreased by the same factor.

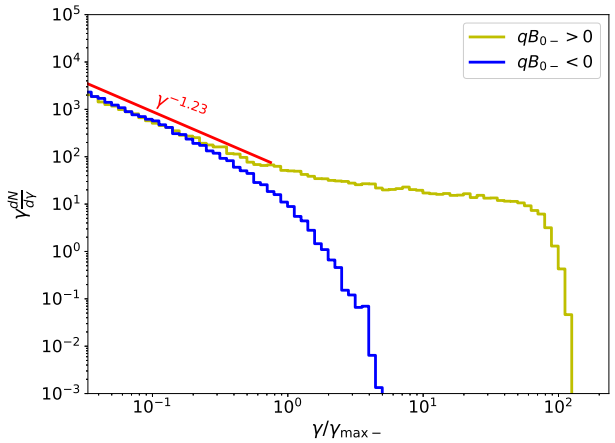

Figure 4: Particle spectra in a cylindrically symmetric magnetic field. Here we consider weak scattering in the upstream, $\nu_{0+} = 10^{-4}\nu_{0-}$. The yellow and blue histograms show results for $qB_{0-} > 0$ and $qB_{0-} < 0$, respectively, plotted as functions of $\gamma/\gamma_{\mathrm{max}-}$ ($\gamma_{\mathrm{max}-} = 3\times10^4$). The simulations were run until a steady state was reached. For $qB_{0-} > 0$ a cut off appears at roughly the confinement limit, $\gamma \approx \rho_{\mathrm{max}} = 10^7$. .

4. Conclusions

Using the Monte-Carlo test-particle simulations, we study particle acceleration at relativistic shocks considering two configurations of regular magnetic fields. We demonstrate that, lacking strong scattering downstream, particle acceleration at relativistic shocks can still be effective. In the perpendicular case, e.g., a uniform field perpendicular to the shock normal, particle acceleration would be saturated only when particles become magnetized on both sides of the shock. Hence, with a strong scattering upstream, the maximum achievable energy can exceed the widely-held *downstream magnetized limit*.

In the cylindrical case, the drift motion caused by the field curvature plays an important role in particle acceleration. For particles with favorable charges, such a drift motion can enhance the acceleration efficiency, harden the produced spectrum and increase the maximum energy to the confinement limit of the system, while for particles with opposite charges, the acceleration efficiency shrinks and hence softens the spectrum.

Because of the spectrum hardening, the interaction between high-energy particles and background plasma becomes important, which unfortunately cannot be included in the test-particle code. Therefore, Kinetic particle-in-cell (PIC) simulations would be necessary to study such an effect.

References

[1] Kirk, J. G. & Duffy, P. 1999, Journal of Physics G Nuclear Physics, 25, R163. doi:10.1088/0954-3899/25/8/201

[2] Kirk, J. G. & Reville, B. 2010, The Astrophysical Journal Letter, 710, L16. doi:10.1088/2041-8205/710/1/L16

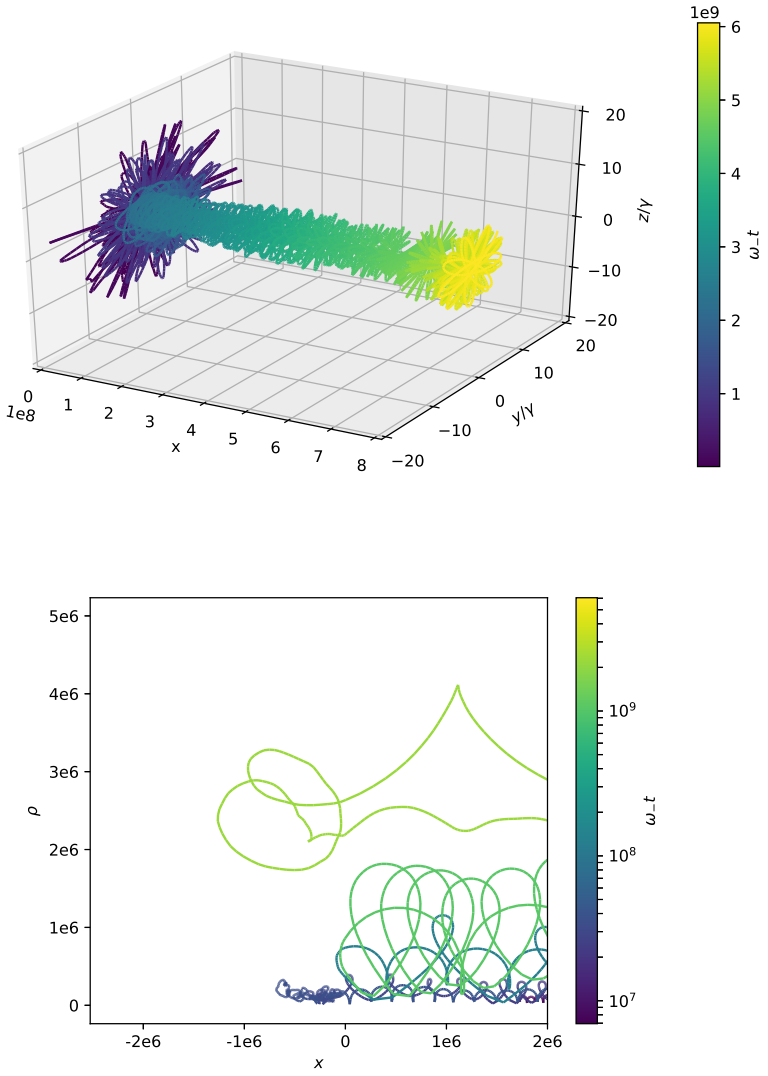

Figure 5: Trajectory in the shock rest frame of a particle with $qB_{0-} > 0$ and Lorentz factor above $\gamma_{\max -}$. Top panel: Particle trajectory in 3-dimensional space before escaping from the boundary $\rho_{\max}$ in the upstream region. Bottom panel: the trajectory in the x–ρ-plane near the shock front.

[3] Achterberg, A., Gallant, Y. A., Kirk, J. G., et al. 2001, Mon. Not. R. Astron. Soc., 328, 393. doi:10.1046/j.1365-8711.2001.04851.x

[4] Huang, Z.-Q., Kirk, J. G., Giacinti, G., et al. 2022, The Astrophysical Journal, 925, 182. doi:10.3847/1538-4357/ac3f38

[5] Huang, Z.-Q., Reville, B., Kirk, J. G., et al. 2023, Mon. Not. R. Astron. Soc., 522, 4955. doi:10.1093/mnras/stad1356

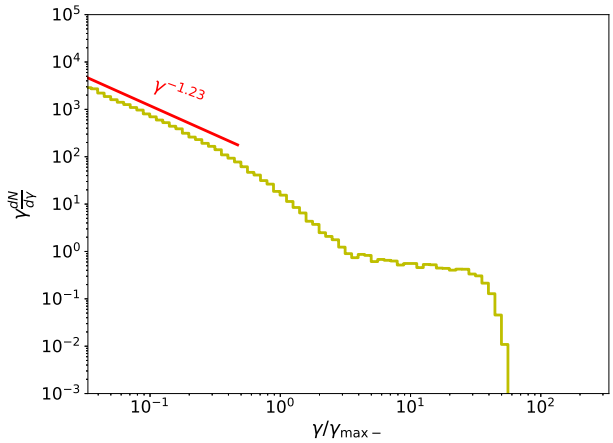

Figure 6: The spectrum for particles with $qB_{0-} > 0$ and the same parameters as in fig 4, but with an upper limit on the jet radius reduced by a factor of 2, i. e., $\rho_{\max} = 5 \times 10^6$. Also, particles are now injected with a uniform distribution in ρ between the axis $\rho = 0$ and $\rho_{\max}$. Only those that reach $\gamma \approx \gamma_{\max -}$ when close to the axis are accelerated further.

[6] Kirk, J. G., Reville, B., & Huang, Z.-Q. 2023, Mon. Not. R. Astron. Soc., 519, 1022. doi:10.1093/mnras/stac3589